

Deuterium NMR Characterization of 1,2-Polybutadiene Local Dynamics in Dilute Solution

Wei Zhu and M. D. Ediger*

Department of Chemistry, University of Wisconsin, Madison, Wisconsin 53706

Received April 13, 1995; Revised Manuscript Received August 3, 1995*

ABSTRACT: Variable temperature ^2H NMR T_1 measurements have been performed on perdeuterated atactic 1,2-polybutadiene (1,2-PB) at two Larmor frequencies in five solvents: toluene, dodecane, hexadecane, *cis*-decalin, and squalene. A model independent correlation time for C–D vector reorientation, $\langle\sigma\rangle$, is determined from the T_1 data. The hydrodynamic Kramers' equation in the high friction limit cannot describe the viscosity and temperature dependence of $\langle\sigma\rangle$. In contrast, $\langle\sigma\rangle$ has an apparent power law viscosity dependence with an exponent of 0.43. Accounting for this viscosity dependence, the average potential energy barrier between conformational states is determined to be 14 kJ/mol. T_1 data have also been fitted to various relaxation time distributions. Unimodal distributions cannot fit the data while bimodal distributions are successful. This indicates that the orientational relaxation of C–D vectors occurs on two well separated time scales. These two features of the relaxation time distribution are presumably caused by librations and conformational transitions. The modification of solvent dynamics caused by the addition of 1,2-PB is also discussed.

I. Introduction

The local segmental dynamics of synthetic polymers play an important role in determining the mechanical properties of these materials. In bulk polymers, dynamics on the scale of a few repeat units control the glass transition temperature, T_g . Dilute solution studies of local polymer dynamics allow the mechanism of conformational transitions to be studied without complications from chain–chain interactions. In addition, the potential energy barrier between different conformational states can be evaluated from careful experiments. This barrier height is expected to have a significant influence on T_g . Thus the study of local polymer dynamics in dilute solution may play an important role in understanding structure/property relationships for synthetic polymers.

We report here ^2H NMR measurements of the local dynamics of perdeuterated atactic 1,2-polybutadiene (1,2-PB, also known as poly(vinylethylene)). Variable temperature measurements within the range 220–420 K were performed in five solvents at two Larmor frequencies. These results allow us to characterize three different aspects of local dynamics in 1,2-PB solutions, as described in the following paragraphs. In the course of this description, the motivation for performing these experiments on 1,2-PB will become clear.

We first address how the solvent influences 1,2-PB local dynamics in dilute solution. Kramers' equation^{1,2} is usually assumed to be an accurate description of polymer–solvent coupling. In the high-friction limit and when specific solvent–polymer interactions are unimportant, the hydrodynamic Kramers' equation predicts that local polymer dynamics should scale linearly with the solvent viscosity η . The applicability of Kramers' equation to this problem has been called into question by recent ^{13}C NMR studies. For polyisoprene in dilute solution, the time integral of a C–H vector orientation autocorrelation function was found to vary as $\eta^{0.41}$, while an $\eta^{0.33}$ dependence was observed for *cis*-polybutadiene.^{3,4} The explanation presented for these deviations from Kramers' behavior indicates that

the size of the side group should be one important variable in determining the viscosity dependence of local dynamics. Thus we desired to study the local dynamics of 1,2-PB because of its somewhat larger side group. We observe an $\eta^{0.43}$ dependence for C–D vector reorientation in 1,2-PB whether the viscosity is varied by changing temperature or solvent.

We also address the mechanism of local polymer dynamics in dilute solutions of 1,2-PB. Dejean de la Batie et al.⁵ reported that the orientational relaxation of C–H vectors in poly(vinyl methyl ether) occurs on two well-separated time scales. Later similar results were obtained for polyisoprene,^{6,7} 1,4-polybutadiene,⁶ poly(propylene oxide),⁸ and poly(1-naphthylalkyl acrylate)s.⁹ Our results indicate that the same conclusion applies to C–D vector reorientation in 1,2-PB. The faster time scale motions are believed to be librational motions which occur near the minima of the torsional potentials. The extent of these librational motions is compared for various polymers.

The third aspect of 1,2-PB local dynamics discussed in this paper concerns the modification of solvent dynamics caused by the addition of a small amount of 1,2-PB. Recent work has shown that the addition of polymer can either speed up or slow down solvent dynamics.^{10–15} Modified solvent dynamics can then influence the dynamics of the polymer on all length scales, altering the intrinsic viscosity of the polymer and the viscoelastic properties of the polymer solution.¹⁰ An equation relating the extent of the modification of solvent dynamics to the ratio of time scales for polymer and solvent motions has been proposed by Gisser and Ediger.¹¹ With the ^2H T_1 data reported here and previously published results by Amelar et al.¹³ this equation can be tested for 1,2-PB. While the equation does not provide a quantitative description of the experimental results, it qualitatively predicts the trend observed in the 1,2-PB experiments relative to those observed for solutions of polyisoprene, polystyrene, and 1,4-polybutadiene.

II. Experimental Section

Materials. Perdeuterated atactic 1,2-polybutadiene (1,2-PB) was a gift from Prof. Julia Kornfield. This polymer has $M_n = 69\,000$ with $M_w/M_n = 1.36$; it contains 93% 1,2-vinyl units

* Abstract published in *Advance ACS Abstracts*, October 15, 1995.

Table 1. Viscosity of Squalene

temp (K)	viscosity (cP)	temp (K)	viscosity (cP)
367.0	3.0	405.9	1.8
377.4	2.6	416.7	1.6
392.4	2.1		

and 7% 1,4 units. Detailed information about the synthesis and properties of this polymer may be found elsewhere.¹⁶ It has been previously established that when the molecular weight of flexible polymers exceeds roughly 10 000, local polymer dynamics are independent of molecular weight.^{17,18} Thus we expect that the results reported here are typical of high molecular weight 1,2-PB chains.

Five solvents were used in this study: toluene, *n*-dodecane, *n*-hexadecane, *cis*-decalin, and squalene. They were all purchased from Aldrich and used as received (purity $\geq 98\%$). Except as noted below, the viscosities of the solvents are reported in the literature.^{19–23} The viscosity of squalene at high temperature was measured using a Cannon–Fenske capillary flow viscometer. These results are shown in Table 1.

We attempted NMR measurements over as wide a range of temperature and solvent viscosity as possible. Except for the case of *cis*-decalin, the high-temperature limit for each solvent was set either by the solvent boiling point or the NMR probe (limited to 425 K). 1,2-PB/*cis*-decalin solutions phase separated above 395 K, so data from this solvent were only collected below this temperature. At 373 K, the five solvents cover a viscosity range of more than 1 decade. Use of more viscous solvents would not allow extreme narrowing conditions to be achieved over a significant temperature range.

The polymer concentration in all solutions was $1.8 \pm 0.3\%$ (w/w). Oxygen was eliminated from the solutions by several freeze–pump–thaw cycles. Samples were then sealed under vacuum. Previous work has indicated that the spin–lattice relaxation time is independent of polymer concentration when the concentration is less than 15%.^{17, 18, 24} Thus the T_1 measurements reported here reflect dynamics for the low concentration limit.

A few ^{13}C NMR T_1 measurements were performed on normal 1,2-PB in toluene- d_8 . This polymer was a gift from Prof. Frank Bates. It has an average molecular weight of about 70 000 and 98% 1,2-vinyl units. For these ^{13}C NMR experiments, the 1,2-PB concentration was 10%.

NMR Measurements. Deuterium T_1 s were measured on Bruker AM-500 and AC-100 spectrometers at 76.86 and 15.37 MHz ^2H Larmor frequencies, respectively. A standard inversion–recovery–FID pulse sequence was employed. The temperature was stable within 2 K. T_1 results are generally accurate within 5%.

Figure 1 shows ^2H spectra of perdeuterated 1,2-PB in toluene at 15.37 and 76.86 MHz. Spectra in other solvents are similar. At 76.86 MHz, four distinct peaks are seen; these have been previously assigned.²⁵ Only two peaks are resolved at 15.37 MHz, corresponding to deuterons on the chain backbone and side group. In order to compare T_1 results at different Larmor frequencies, we calculated T_1 s for the chain backbone deuterons at 76.86 MHz by a weighted average of the T_1 s of the two individual backbone peaks. In order to check the weight average method, sometimes 60–100 Hz line broadening was used to collapse the backbone peaks; T_1 s were then calculated using the collapsed peak. The results from these two methods were found to agree within a few percent. Side-group T_1 s at 76.86 MHz were also weight averaged when making a comparison with the 15.37 MHz data.

Data Analysis. Deuterium nuclear magnetic moments are relaxed by electric quadrupole coupling. T_1 is related to the reorientation of C–D vectors by^{26,27}

$$\frac{1}{T_1} = \frac{3}{10} \pi^2 (e^2 q Q / h)^2 (1 + \xi) [J(\omega_D) + 4J(2\omega_D)] \quad (1)$$

where $\omega_D/2\pi$ is the Larmor frequency. The ^2H quadrupole coupling constant $e^2 q Q / h$ for the two types of backbone deuterons should be very similar; we use a value of 172

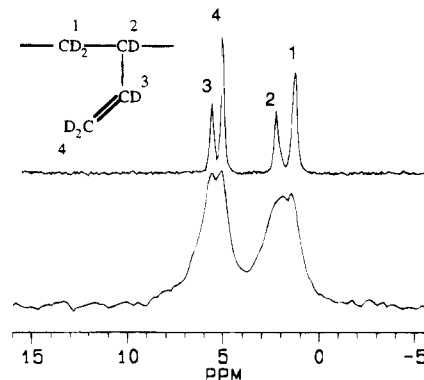


Figure 1. ^2H spectra of perdeuterated 1,2-PB in toluene at 76.86 MHz (top) and 15.37 MHz (bottom). The temperature is 354 K.

KHz.^{18,28,29} $e^2 q Q / h$ for the side-group deuterons is chosen to be 190 MHz.^{28,29} The uncertainty in these numbers is expected to be less than 5% and 8%, respectively. The symmetry parameter ξ expresses the departure of the electric field gradient from cylindrical symmetry. For deuterium in C–D bonds, ξ is known to be close to zero; we set $\xi = 0$ when using eq 1.

The spectral density function $J(\omega)$ is defined by

$$J(\omega) = \frac{1}{2} \int_{-\infty}^{+\infty} G(t) e^{i\omega t} dt \quad (2)$$

Here $G(t)$ is the second-order orientation autocorrelation function for a C–D bond:

$$G(t) = \frac{1}{2} \langle 3(\mathbf{e}_x(0) \cdot \mathbf{e}_x(t))^2 - 1 \rangle \quad (3)$$

In this equation, $\mathbf{e}_x(t)$ is a unit vector in the direction of the C–D bond at time t . The brackets indicate an ensemble average.

Molecular motion may be characterized by a model independent quantity, $\langle \sigma \rangle$,³⁰ which is the time integral of the correlation function $G(t)$:

$$\langle \sigma \rangle = \int_0^\infty G(t) dt \quad (4)$$

T_1 is inversely proportional to $\langle \sigma \rangle$ in the extreme narrowing regime:

$$\frac{1}{T_1} = \frac{3}{2} \pi^2 (e^2 q Q / h)^2 \langle \sigma \rangle \quad (5)$$

One criterion for the extreme narrowing region is that T_1 is independent of the Larmor frequency. Another criterion often used is that $T_1 = T_2$. Because T_2 is sensitive to very low frequency motions, for polymers T_1 is generally not equal to T_2 .^{18,31} When the first criterion is met but the second is not, we can use eq 5 to calculate $\langle \sigma \rangle$ with the understanding that it represents the average relaxation time for all fast motions, i.e., the upper limit of integration in eq 4 is replaced by $1/(\omega_D)$.

It is important to note that $\langle \sigma \rangle$ is not based on any assumption about the shape of the correlation function. $\langle \sigma \rangle$ is an integral, not a time constant, for a particular type of molecular motion which might be assumed in a molecular model. The conclusions drawn in section III are independent of whatever model might be used to fit $G(t)$.

We began this investigation using natural abundance ^{13}C NMR measurements on nondeuterated atactic 1,2-PB. The mixed tacticity results in many small peaks in the ^{13}C spectrum and, as a result, our ^{13}C T_1 measurements on 10% 1,2-PB in solution were quite unreliable. Nevertheless, $\langle \sigma \rangle$ values obtained from this preliminary investigation agree with those obtained from ^2H NMR measurements to within 30%. We will only discuss the ^2H T_1 results in the rest of this paper.

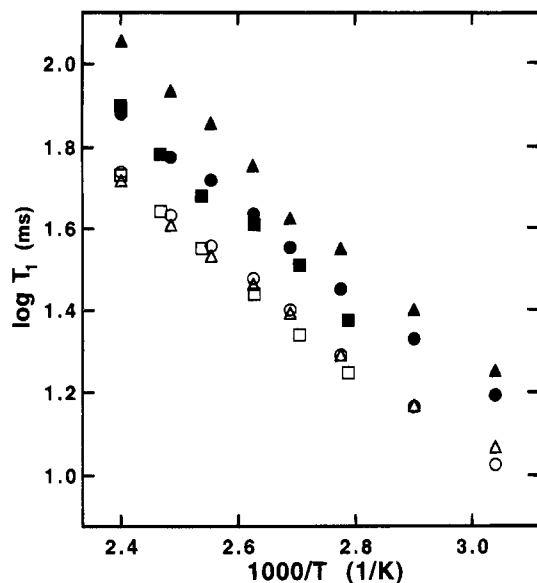


Figure 2. ^2H T_1 vs temperature for perdeuterated 1,2-PB in hexadecane. Backbone deuterons are shown as open symbols while side-group deuterons are shown as filled symbols: side-group methine carbon at 76.86 MHz (\blacktriangle); side-group methylene carbon at 76.86 MHz (\bullet); backbone methine carbon at 76.86 MHz (\triangle); backbone methylene carbon at 76.86 MHz (\circ); side-group deuterons at 15.37 MHz (\blacksquare); backbone deuterons at 15.37 MHz (\square). Backbone C–D motions meet the extreme narrowing condition since T_1 data at two Larmor frequencies agree with each other.

The superior signal-to-noise obtained in the ^2H experiments results primarily from the greater concentration of active nuclei and the shorter relaxation times (which allow efficient signal averaging). A more subtle advantage of ^2H measurements for this study is that the extreme narrowing condition can be met over a wider range of temperature. This is because the dominant term in eq 1 is $J(2\omega_D)$. In a similar equation for ^{13}C T_1 , the dominant term is $J(\omega_C + \omega_H)$.¹⁸ At the same magnetic field strength, $\omega_C + \omega_H$ is approximately 4 times $2\omega_D$. Thus, since we wanted to work in the extreme narrowing regime, ^2H measurements allowed the study of molecular motions 4 times slower than would have been possible with ^{13}C . One disadvantage of ^2H NMR is that NOE measurements are not applicable; these provide valuable information about molecular motions.

III. Viscosity and Temperature Dependence of Correlation Times

Figure 2 shows ^2H T_1 s for deuterated 1,2-polybutadiene (1,2-PB) in hexadecane as a function of temperature. T_1 s for side-group deuterons (filled symbols) are significantly longer than T_1 s for backbone deuterons (open symbols). Accounting for the differences in quadrupole coupling constants, side-group C–D vectors reorient about twice as fast as backbone C–D vectors, in qualitative agreement with our expectations. For temperatures above 350 K, T_1 s for backbone deuterons at 15.37 and 76.86 MHz agree within 10%, indicating that the extreme narrowing condition is fulfilled. This could not be checked at lower temperatures since the backbone and side-group peaks seen at higher temperatures in the 15.37 MHz ^2H spectrum coalesced into a broad single peak. In contrast, T_1 s for side-group deuterons at 15.37 MHz are more than 20% smaller than the average side-group T_1 s at 76.86 MHz. This means that side-group motions are further away from extreme narrowing conditions than the backbone motions, which is interesting yet puzzling. Because the main interest of this paper is polymer backbone motions,

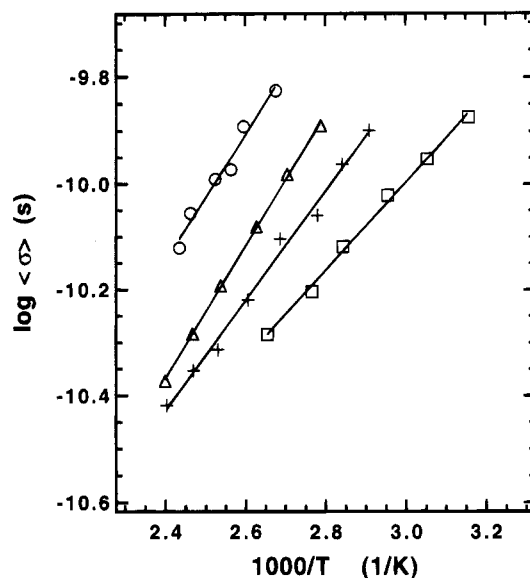


Figure 3. Correlation times for 1,2-PB backbone C–D vector reorientation in different solvents: squalene (\circ); hexadecane (\triangle); dodecane ($+$); toluene (\square). Data were calculated from T_1 at 15.37 MHz.

we will not further discuss the side group. T_1 data for side-group deuterons are provided as supporting information.

Although our measurements were done over different temperature ranges in different solvents, the dependence of T_1 on Larmor frequency for all solvents is the same as the behavior shown for hexadecane in Figure 2. Because T_1 s for backbone deuterons show no significant difference at two Larmor frequencies, we assume that all the T_1 s at 15.37 MHz are in the extreme narrowing region. A calculation described in section IV provides additional justification for this assumption. Figure 3 shows correlation times for four solvents calculated with eq 5 using 15.37 MHz T_1 data. At a given temperature, higher viscosity solvents such as squalene and hexadecane naturally show a larger $\langle\sigma\rangle$, indicating slower motions.

The 76.86 MHz T_1 data in Figure 2 show that the two types of deuterons in the backbone have very similar T_1 s. Since the quadrupole coupling constants are the same, both types of C–D vectors in the chain backbone reorient at essentially the same rate. Similar conclusions have been reached about other vinyl polymers which have been investigated using ^{13}C T_1 experiments.^{5,17,18,32} In these cases the backbone methylene and methine C–H vectors have been found to reorient at approximately the same rate. This is also true for polymers with backbone heteroatoms, such as poly(styrene oxide),³³ poly(phenyl thiirane),³⁴ and poly(styrene peroxide).³⁵ In polymers with relatively flexible and rigid parts in their backbone, such as 1,4-polyisoprene^{3,6,36} and 1,4-polybutadiene,^{4,6,37} backbone methylene and methine C–H vectors have been found to reorient at different rates.

Failure of the Kramers' Approach. Kramers' theory^{1,2} calculates the transition rate for a particle passing over an energy barrier under the influence of Gaussian random forces. The equation usually used to describe the temperature and viscosity (η) dependence of the correlation time in dilute solution is^{17,24,38,39}

$$\langle\sigma\rangle = A\eta \exp\left(\frac{E_a}{RT}\right) \quad (6)$$

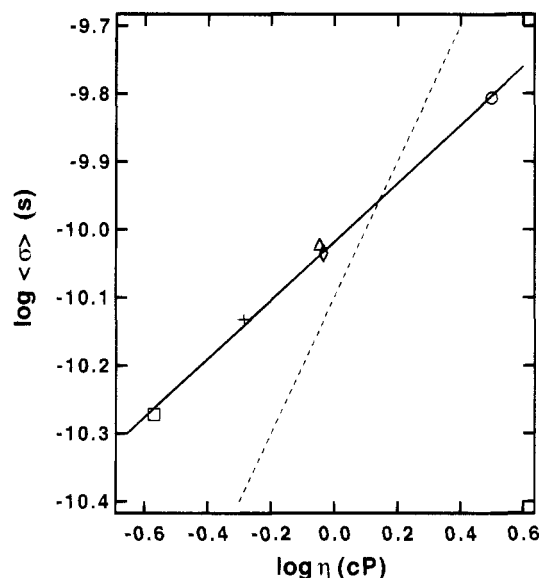


Figure 4. Correlation times for 1,2-PB backbone C-D vector reorientation plotted against solvent viscosity at 373 K. Different solvents are indicated by the symbol codes in Figure 3. The diamond is derived from T_1 s in *cis*-decalin at 76.86 MHz. The solid line has a slope of 0.43. A dashed line with a slope of 1 (high friction Kramers' prediction) is also shown for comparison.

Here A is a constant and E_a is the height of the potential energy barrier between two conformational states. Equation 6 can be obtained from Kramers' theory by making three assumptions: (1) the high-friction limit of the Kramers' equation is appropriate, (2) Stokes' law is used to relate the microscopic friction to the shear viscosity of the solvent at zero frequency, and (3) the correlation time for a vector fixed in the polymer backbone is inversely proportional to the conformational transition rate.

Equation 6 can be tested in two ways using the data shown in Figure 3. Figure 4 shows $\langle\sigma\rangle$ for 1,2-PB as a function of solvent viscosity at 373 K. The data show a slope of 0.43 (solid line) in contrast to the linear viscosity dependence predicted by eq 6 (dashed line). The fact that all solvents lie on a single straight line indicates that specific interactions are not responsible for the deviation from eq 6. We further note that molecular shape does not seem to affect $\langle\sigma\rangle$ as an independent variable. We purposely chose *cis*-decalin and hexadecane as two of the five solvents because they have almost the same viscosity but much different shapes. Essentially identical local dynamics are observed in these two solvents.

A further test of eq 6 may be performed by varying temperature. Figure 5 plots $\log(\langle\sigma\rangle/\eta)$ against inverse temperature. According to Kramers' theory, all solvents should fall on one straight line. In contrast, the four solvents fall on four different lines. While one might argue that the pre-exponential factor A could be different for different solvents, a systematic variation with the solvent viscosity is suspicious. In addition, use of eq 6 gives potential barrier heights of 7–9 kJ/mol for 1,2-PB. This is too small considering that the energy barrier for polyethylene is around 12 kJ/mol and that 1,2-PB and polyethylene have the same backbone structure.⁴⁰ Thus we conclude that the local dynamics of 1,2-PB in dilute solution cannot be rationalized using eq 6. Indeed, the use of eq 6 to estimate the energy barrier in 1,2-PB and other polymers may lead to serious error.

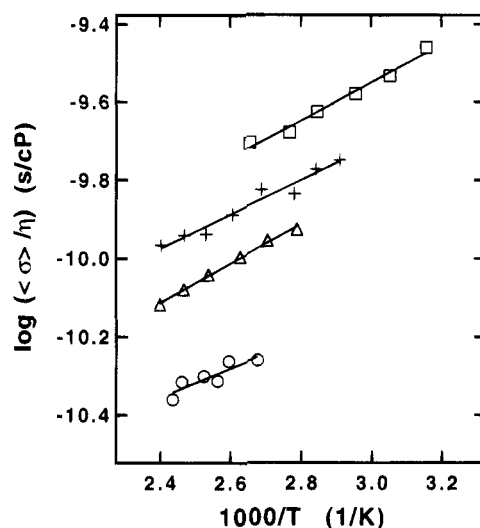


Figure 5. A test of Kramers' theory in the high friction limit using C-D vector reorientation times in various solvents. Solvent symbols are the same as in Figure 3. Different solvents have different lines, which suggests that the high friction Kramers' equation cannot describe 1,2-PB local dynamics in dilute solution.

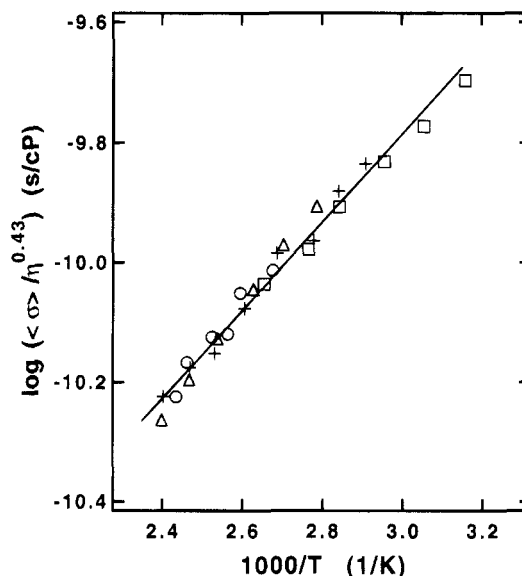


Figure 6. A test of a power law viscosity dependence (eq 7) for C-D vector reorientation in various solvents. Solvent symbols are the same as in Figure 3. The superposition indicates that eq 7 is a reasonable description of the experimental data.

Nonlinear Viscosity Dependence. It has previously been observed that the local dynamics of polyisoprene³ and *cis*-polybutadiene⁴ can be described by a power law viscosity dependence of the form

$$\langle\sigma\rangle = A\eta^\alpha \exp\left(\frac{E_a}{RT}\right) \quad (7)$$

Figure 4 illustrates that eq 7 adequately describes the viscosity dependence of 1,2-PB local dynamics at 373 K if $\alpha = 0.43$. The temperature dependence of eq 7 may be tested in a manner similar to Figure 5. The result is shown in Figure 6. Data from four solvents fall close to a common line. The slope of this line gives a potential barrier height of 14.1 kJ/mol. Careful inspection of Figure 6 indicates that various solvents systematically differ from the average behavior. Such deviations

Table 2. Viscosity Exponent for Dilute Solution Local Dynamics of Various Polymers

	α	ref (data; analysis)
<i>cis</i> -1,4-polybutadiene	0.33	4; 4
polybutadiene (mixed microstructure)	0.36–0.39	4; 4
polyisoprene	0.41	3; 3
1,2-polybutadiene	0.43	this work
poly(ethylene oxide)	0.67–0.69 ^a	39; 3
poly(vinyl chloride)	0.7–1.0 ^b	59; 4
polystyrene	≈1.0 ^c	24, 60, 61; 11
poly(<i>p</i> -chlorostyrene) ^d	1.0 ^c	38
poly(1-naphthylmethyl acrylate)	1.0 ^e	62; 62

^a Data at only one temperature. ^b Depends upon assumptions about specific interactions. ^c Data cover a narrow viscosity range. ^d Dielectric relaxation measurements. ^e Model dependent, from the fitting of the DLM distribution.

correspond to an activation energy range of 12–17 kJ/mol. Although not a perfect description, the power law viscosity dependence does provide a reasonable fit for all the 1,2-PB data.

Why is the Kramers' approach inconsistent with experimental results on the local dynamics of 1,2-PB? The answer lies either in the failure of Kramers' equation itself or in the assumptions which are made when deriving eq 6 from the Kramers' equation. It has previously been argued that the problem is unlikely to be caused by the high friction assumption⁴¹ or by the use of Stokes' law to connect friction and viscosity.⁴ The most likely explanation for the failure of eq 6 lies in the derivation of the Kramers' equation from the Langevin equation.⁴ The Langevin equation is an approximate description of a system which is accurate only if there exists a significant separation of time scales between system and bath dynamics. In this problem, the polymer chain is the system and the solvent is the bath. Thus, the validity of the Kramers' treatment of local polymer dynamics depends upon whether the relevant chain motions are significantly slower than the relevant solvent motions. It has previously been shown that this separation of time scales does not exist in dilute solutions of polyisoprene and 1,4-*cis*-polybutadiene.^{3,4} In the latter case, solvent rotation times can be an order of magnitude longer than correlation times for local polymer dynamics. While we have not made such a comparison in 1,2-PB solutions, it seems likely that the similar behavior of polyisoprene, 1,4-*cis*-polybutadiene, and 1,2-PB has a common origin. In support of this conclusion, we note that a functional form similar to eq 7 has been obtained theoretically for isomerization rates when the solvent is treated as viscoelastic.⁴²

It is also possible that the seemingly innocuous assumption of inverse proportionality between transition rates and correlation times is in error. Some computer simulations can be interpreted to support this possibility.^{43,44} Molecular dynamics simulations in our laboratory have indicated that this assumption breaks down when comparing local dynamics in solutions and melts.⁴⁵ Further investigation is required to determine whether this assumption fails when local dynamics are compared in a series of solvents. Our current speculation is that changes in the relationship between transition rates and correlation times do not account for the nonlinear viscosity dependence shown in Figure 4.

Comparison to Other Polymers. From the above analysis we expect that non-Kramers' behavior will be observed for polymers with relatively fast local dynamics. Table 2 lists viscosity exponents for a number of

different polymers. It has previously been suggested³ that the exponent α should depend upon several factors including the size of the isomerizing unit. Larger isomerizing units should lead to α being closer to 1. Although we cannot rationalize all the results in Table 2, certain trends can be explained in these terms. For example, adding a methyl group to 1,4-polybutadiene to create polyisoprene increases α by approximately 0.08. The value of α for vinyl polymers increases with the size of the side group, with 1,2-PB having $\alpha = 0.43$ and poly(1-naphthylmethyl acrylate) having $\alpha = 1$.

IV. Correlation Function Shape

The shape of the correlation function $G(t)$ provides some insight into the mechanism of C–D vector reorientation (see eq 3). If C–D vectors underwent isotropic rotational diffusion, then $G(t)$ would be a single exponential with a characteristic relaxation time, τ . In general, $G(t)$ is nonexponential and can be described by a distribution of relaxation times, $F(\tau)$. $F(\tau)$ and $G(t)$ are related by a Laplace transform:

$$G(t) = \int_0^\infty F(\tau) e^{-t/\tau} d\tau \quad (8)$$

Over the past few decades many different distributions have been proposed for $F(\tau)$.^{18,31} These include empirical equations such as Cole–Cole,⁴⁶ $\log \chi^2$,⁴⁷ and Fuoss–Kirkwood⁴⁸ distributions, which do not involve any assumption about the reorientation mechanism. Alternatively, $G(t)$ obtained by assuming a particular mechanism of reorientation can be inverse Laplace transformed to obtain $F(\tau)$. This has been done, for example, with the Hall–Helfand⁴⁹ and Jones–Stockmayer⁵⁰ models. In this paper we will not attempt to distinguish between specific mechanisms. Rather, discussion will be focused on what features in the relaxation time distribution are essential to adequately describe backbone C–D or C–H vector reorientation.

Many different relaxation time distributions have been fit to experimental data. A major constraint can be placed on the fitting process if the shape of the distribution is known to be temperature independent. Some authors have used this constraint^{5,6,8} while others have not.⁵¹ Thus before we determine what kind of distribution functions can best describe our data, we must decide if the relaxation time distribution changes shape with temperature.

Temperature-Frequency Superposition. Guillermo et al. have proposed a model independent temperature–frequency superposition method to test if the distribution of relaxation times is temperature dependent.⁵² This superposition will be successful only if all the relaxation times in the vicinity of $1/\omega_D$ have the same temperature dependence (which means that the shape of $F(\tau)$ on a log scale is independent of temperature). Such a superposition of our data is presented in Figure 7. Equation 7 with $\alpha = 0.43$ and $E_a = 14.1$ kJ/mol was used to construct the abscissa. Unfortunately, it was not possible to extend the 15.37 MHz data through the T_1 minimum due to the overlap of backbone and side-group ^2H peaks at low temperature. Thus we cannot use this plot in the manner suggested by Guillermo et al.

There is indirect evidence in Figure 7 which supports the use of an $F(\tau)$ with a temperature independent shape. The value of T_1 at the T_1 minimum is determined by the width of the relaxation time distribution.^{5,7} A narrow distribution gives a sharp and deep minimum

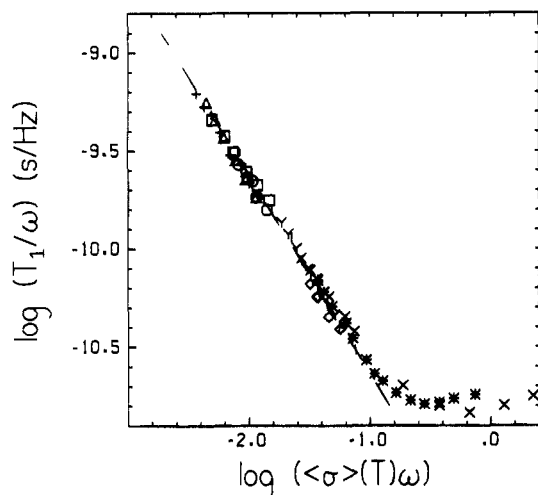


Figure 7. Frequency-temperature superposition of 1,2-PB backbone ^2H T_1 at two Larmor frequencies in five solvents: toluene at 76.86 MHz (\times); *cis*-decalin at 76.86 MHz (\diamond); dodecane at 76.86 MHz (Y); squalene at 76.86 MHz ($*$); hexadecane at 76.86 MHz (I). Solvent symbols for 15.37 MHz data are the same as in Figure 3.

while a wide distribution gives a broad and elevated minimum. As shown in Figure 7, the value of T_1 for 1,2-PB dynamics in toluene and squalene at 76.86 MHz is nearly the same (within 10%). Since their T_1 minima occur at quite different temperatures (240 K in toluene; 305 K in squalene), it is reasonable to conclude that the distribution of relaxation times is temperature independent. The lack of superposition for the two different solvents is presumably due to the inability of eq 7 to describe precisely the temperature dependence in each solvent with a single set of parameters. This inadequacy was previously mentioned in connection with Figure 6.

Temperature-frequency superposition has been successfully demonstrated for other polymers. Guillermo et al.⁵² have been able to superpose T_1 s at different Larmor frequencies in bulk 1,4-polybutadiene. Gisser et al.⁷ have successfully superposed T_1 data of polyisoprene in toluene. Recently, Spyros et al.⁹ found that this superposition is possible for poly(1-naphthylalkyl acrylate)s. On the basis of these results and the indirect evidence from the previous paragraph, we will assume that the relaxation time distribution has a temperature independent shape in the following discussion.

We note one final point about Figure 7. The 15.37 MHz data are on the same straight line as the 76.86 MHz data above the T_1 minimum. The slope of that line is -1 . This is another indication that T_1 is not a function of Larmor frequency in this region and the 15.37 MHz data are in the extreme narrowing limit within the experimental accuracy.

Unimodal Distributions. What kind of relaxation time distribution can best describe our data given the constraint that the shape of $F(\tau)$ is temperature independent? The fitting procedure used is the same as in ref 53; the temperature dependence of the relaxation times is given by eq 7 with $\alpha = 0.43$ and $E_a = 14.1$ kJ/mol. We first consider unimodal distributions of relaxation times. In Figure 8, ^2H T_1 values for 1,2-PB in squalene are plotted against $1000/T$ along with the best fit to the $\log \chi^2$ distribution. Clearly the fit is not very good. The experiments show a minimum T_1 of 8 ms at 76.86 MHz while the fit shows a minimum of 5 ms. The 5% uncertainty in e^2qQ/h cannot explain such a differ-

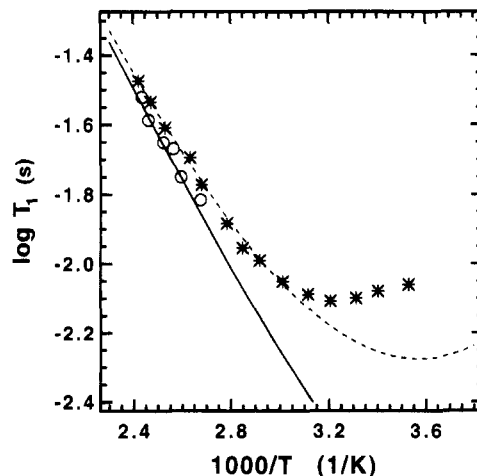


Figure 8. Best fit of the $\log \chi^2$ distribution to backbone ^2H T_1 s of 1,2-PB in squalene. The points are experimental T_1 s at 15.37 MHz (\circ) and 76.86 MHz ($*$). The curves are calculated from the $\log \chi^2$ distribution with $p = 38$ and $b = 1000$: 15.37 MHz ($-$) and 76.86 MHz ($- -$).

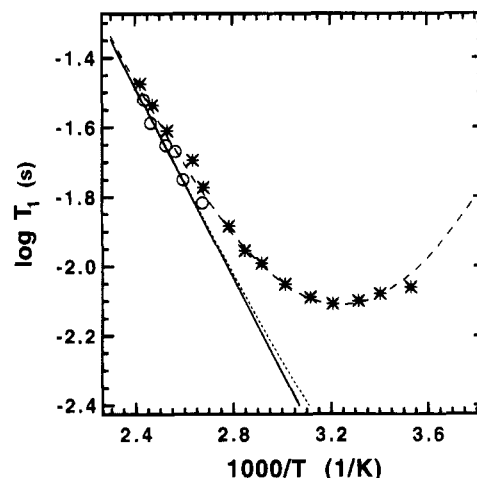


Figure 9. Best fit of the modified $\log \chi^2$ distribution. The points are the same as in Figure 8. The curves are calculated using a $\log \chi^2$ distribution ($p = 100$ and $b = 1000$) plus a single relaxation time. The relative weights of these two are 0.58: 0.42. The dashed line is the calculation for 76.86 MHz. The dotted line is for 15.37 MHz and the solid line is for zero frequency.

ence. We have also tried to fit these data to a Cole-Cole distribution. Again we find that the minimum T_1 in the best fit is much lower than the experimental data.

Other investigators have reported the inability of unimodal distributions to fit NMR T_1 data for several different polymers.^{5-7,9} In each case, unimodal distributions could not account for the value of T_1 at the minimum. This has been interpreted as indicating the existence of very fast motions which occur at frequencies much higher than the Larmor frequency. Such fast motions lift the minimum of the T_1 data while the separation of the fast motions from the Larmor frequency ensures no change in the shape of the T_1 curve near the minimum.

Bimodal Distributions. Since fits with unimodal distributions of relaxation times were not successful, we attempted fits with bimodal distributions. We modified the $\log \chi^2$ distribution by the addition of a single relaxation time, τ_0 , chosen to be 800 times smaller than the $\bar{\tau}$ values which characterizes the $\log \chi^2$ distribution. Figure 9 illustrates that this function provides a very good fit to the experimental data. The choice of $\bar{\tau}/\tau_0 =$

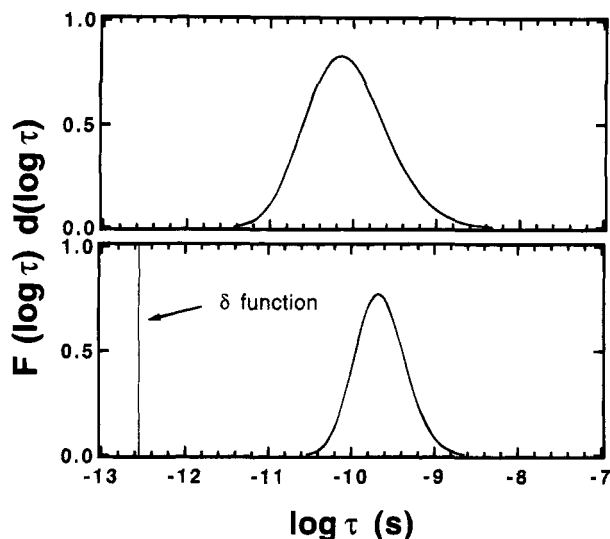


Figure 10. Relaxation time distributions which produced the fits shown in Figures 8 (top panel) and 9 (bottom panel). The essential feature for a successful fit is a bimodal distribution of relaxation times. Thus reorientation of C–D bond vectors occurs on two well-separated time scales. The temperature is 373 K.

800 is fairly arbitrary. As long as this ratio is large, a good fit is always obtained. In the correlation function calculated from this relaxation time distribution (via eq 8), the fast single relaxation time accounts for 42% of the total C–D reorientation. We also attempted to fit our data to other bimodal distributions including the DLM model⁵ (a single relaxation time plus a Hall–Helfand distribution) and a modified Cole–Cole distribution⁷ (a single relaxation time plus a Cole–Cole distribution). These relaxation time distributions can also well describe our data; none of these bimodal distributions provided a significantly better fit than any of the others.

The two relaxation time distributions used in Figures 8 and 9 are shown in Figure 10. The distribution which provides the better fit (bottom panel) has a narrower distribution of relaxation times in the vicinity of $1/\omega_D$ and, in addition, has motions much faster than $1/\omega_D$. As long as there is a clear separation between the fast and the slow motions, and as long as the fast motions account for 42% of the total C–D vector reorientation, a good fit to the T_1 data is expected. Although we represent the fast motions by a single relaxation time in fitting the data, the actual relaxation time distribution of the fast motions is likely to be much more complex. More detailed information about the fast motions can be obtained from higher frequency techniques such as quasi-elastic neutron scattering.⁵⁴

A final piece of information can be obtained from the fit shown in Figure 9. The solid line in this figure shows T_1 calculated at zero frequency using the relaxation time distribution which fits the 15.37 and 76.86 MHz data. The close agreement between this line and the line and data for 15.37 MHz indicate that the 15.37 MHz data are very close to the extreme narrowing limit. This provides further justification for the use of eq 5 in calculating $\langle\sigma\rangle$ from T_1 .

Interpretation of the Relaxation Time Distribution. Our conclusion that C–D vector reorientation occurs on two well-separated time scales in 1,2-PB is consistent with ¹³C NMR studies of other polymers^{5–7,9} which indicate that C–H vector reorientation occurs on two well-separated time scales. It is generally assumed

Table 3. Percentage of Backbone C–H or C–D Correlation Function Decay Due to Librational Motions

polymer and bond	percentage	ref
solution polyisoprene CH	41	7
solution polyisoprene CH ₂ (away from methyl group)	48	7
solution polyisobutylene CH ₂	21	63
solution 1,2-polybutadiene CD and CD ₂	42	this work
solution poly(vinyl methyl ether) (both CH and CH ₂)	40	5
solution PNA ^a CH	22	9
solution PNMA ^b CH	15	9
solution PNEA ^c CH	16	9
bulk <i>cis</i> -polybutadiene CH ₂	46	6
bulk <i>cis</i> -polybutadiene CH	27	6
bulk <i>cis</i> -polyisoprene CH ₂ (closer to methyl group)	40	6
bulk <i>cis</i> -polyisoprene CH ₂ (away from methyl group)	48	6
bulk <i>cis</i> -polyisoprene CH	17	6
bulk poly(vinyl methyl ether) (both CH and CH ₂)	40	5
bulk polyisobutylene CH ₂	21	63
bulk poly(propylene oxide) CH	24	8
bulk poly(propylene oxide) CH ₂	49	8

^a Poly(1-naphthyl acrylate). ^b Poly(1-naphthylmethyl acrylate). ^c Poly(1-naphthylethyl acrylate).

that the fast motions are librations, reflecting the wobbling motion of C–D vectors near the bottom of a torsional potential energy minimum.⁵⁵ These motions are so fast and sufficiently limited in amplitude that they are expected to be roughly independent of solvent viscosity. Recent molecular dynamics computer simulations on polyisoprene confirm several aspects of this picture.^{56,57} Both solution and melt simulations indicate very fast, limited amplitude C–H vector reorientation. Simulations of polyisoprene in toluene show that the fast drop (≈ 1 ps) in $G(t)$ is substantially due to torsional adjustments near torsional potential minima. Simulations of polyisoprene in solution and the melt show that the librational motions are quite insensitive to whether the chain is surrounded by solvent or polymer.

The slower group of motions in the relaxation time distribution occur near $1/\omega_D$ in our experiments on 1,2-PB (see the bottom panel in Figure 10). These motions have usually been interpreted in terms of the crossing of torsional energy barriers, i.e., conformational transitions. We tentatively adopt this interpretation even though the simulations mentioned in the previous paragraph also indicate a possible contribution due to the coupling of small amplitude motion of several neighboring torsions.

For completeness, we mention evidence of a third, much slower process in the relaxation time distribution for C–H or C–D vector reorientation.⁴ A C–D or C–H vector in the backbone of a polymer chain cannot be completely randomized until the entire polymer chain has reoriented. This third portion of $F(\tau)$ probably accounts for (at most) the last few percent of the decay of $G(t)$. NMR T_1 experiments are not very sensitive to these motions and thus they do not appear in Figure 10. Since T_1 data were used to determine $\langle\sigma\rangle$ in section III, the temperature and viscosity dependence of $\langle\sigma\rangle$ is determined mainly by the motions in the vicinity of $1/\omega_D$ which we have interpreted as conformational transitions.

Comparison with Other Polymers. The fitting procedure discussed above indicates that librational motions account for about 42% of the C–D correlation function decay in 1,2-PB. In Table 3 we have compiled

this quantity for various polymers. Much of the data may be rationalized on the basis of steric arguments. Since double bonds are quite rigid, C–H vectors attached to unsaturated carbons naturally tend to have a smaller range of libration. This explains variations in the librational contribution for different C–H vectors in polyisoprene and 1,4-polybutadiene. For the vinyl polymers, side groups create resistance to librational motion in the chain backbone. 1,2-PB and poly(vinyl methyl ether) have side groups of similar size and also have nearly the same librational contribution to the correlation function decay. Poly(1-naphthylalkyl acrylate)s have large side groups and smaller librational contributions. In most cases there is no significant difference between solution and bulk polymers in terms of the contribution of librational motions to the correlation function decay.

V. Modification of Solvent Dynamics

The solvent in a polymer solution has traditionally been viewed as a viscous continuum the properties of which are not affected by the presence of the polymer. Recently it has been shown that the presence of polymer can significantly modify the dynamics of the solvent molecules. In turn, the polymer dynamics can be modified by the change in properties of the surrounding solvent. Interestingly, the polymer can act either to speed up or slow down the solvent dynamics. This phenomenon has been recently reviewed in ref 10.

Gisser and Ediger^{11,58} have presented an empirical equation to describe the extent to which the dynamics of the solvent will be modified by a given polymer:

$$\frac{\partial}{\partial c} \ln \left(\frac{\tau_{\text{soln}}(c, T)}{\tau_{\text{soln}}} \right) \approx Q \log \left(\frac{\tau_{\text{poly}}}{\tau_{\text{soln}}} \right) \quad (9)$$

Here, $\tau_{\text{soln}}(c, T)$ is a time constant characterizing solvent motions at concentration c and temperature T and $\tau_{\text{soln}} = \tau_{\text{soln}}(0, T)$. τ_{poly} is a time constant for local polymer relaxation in dilute solution at temperature T ; it is equivalent to $\langle \sigma \rangle$ in this paper. Q is a constant for a given solvent. Conceptually, eq 9 says that the change in solvent dynamics upon addition of polymer is related to the ratio of the time scales for polymer and solvent motions. "Fast" polymers will cause solvent dynamics to get faster and "slow" polymers will cause solvent dynamics to slow down.

Gisser and Ediger showed that experimental data for three polymers (polystyrene, polyisoprene, and 1,4-polybutadiene) in Aroclor were reasonably described by eq 9 if $Q = 4$ mL/g. One motivation for the current study of 1,2-PB dynamics was that the effect of 1,2-PB addition on solvent dynamics has been characterized by Amelar et al.¹³ The results presented in section III can be used to estimate $\langle \sigma \rangle$ as a function of temperature in Aroclor if we assume that eq 7 is applicable (using $\alpha = 0.43$ and $E_a = 14.1$ kJ/mol). Thus eq 9 can now be tested for a fourth polymer in solution with Aroclor. Amelar et al.³ found that Aroclor rotation was not a function of 1,2-PB concentration from 256 to 276 K; thus the left side of eq 9 is essentially zero. Using eq 7 we find that the right side of eq 9 varies from -12 to -4 mL/g from 256 to 276 K if the above value of Q is assumed.

Clearly eq 9 does not quantitatively describe the modification of Aroclor dynamics by 1,2-PB. This is not surprising, however, since this equation did not quantitatively describe the data for 1,4-polybutadiene, poly-

isoprene, and polystyrene solutions with Aroclor. Equation 9 does predict the correct qualitative effect of 1,2-PB addition relative to the other polymers. Both eq 9 and the experiments indicate that polystyrene slows down Aroclor dynamics while polyisoprene and 1,4-polybutadiene speed up Aroclor dynamics. Both eq 9 and experiments indicate that the effect of 1,2-PB is intermediate between these two groups.

VI. Summary and Concluding Remarks

Deuterium T_1 experiments have been carried out on perdeuterated 1,2-polybutadiene in five solvents at two Larmor frequencies. The comparison of T_1 at two Larmor frequencies indicates that T_1 data at 15.37 MHz are in the extreme narrowing region. The time integral of the backbone C–D orientation autocorrelation function $\langle \sigma \rangle$ has been extracted from the T_1 data. The viscosity and temperature dependence of $\langle \sigma \rangle$ suggest that Kramers' theory is not appropriate for this problem because the relevant polymer and solvent motions do not occur on well-separated time scales.

The local dynamics of 1,2-PB were found to depend upon the solvent viscosity η raised to the 0.43 power. We had anticipated that the vinyl side group on 1,2-PB would significantly increase the viscosity exponent above that observed for polyisoprene ($\eta^{0.41}$). This expectation was based on the observation that the viscosity exponent jumps from 0.33 to 0.41 when a methyl group is added to the 1,4-polybutadiene. The 1,2-PB result suggests that quite large side groups may be required to reach to Kramers' scaling of η^1 . We are currently investigating the viscosity dependence of polystyrene using a much larger range of solvent viscosities than has previously been employed.

Analysis of T_1 data in squalene at two Larmor frequencies reveals that unimodal relaxation time distributions cannot describe the reorientation of backbone C–D vectors. Fast librational motions near the minima of the torsional potential wells have to be added to larger amplitude motions (presumably conformational transitions) in order to obtain reasonable fits. The extent of librational motions in various polymers can be rationalized on the basis of steric arguments.

Acknowledgment. This research was supported by the National Science Foundation through the Division of Material Research, Polymers Program (DMR-9424472). Some NMR experiments were performed in the Instrument Center of the Department of Chemistry, University of Wisconsin. We thank the staff for assistance. We also thank Tom Farrar for use of an NMR spectrometer. We gratefully acknowledge Frank Bates and Julia Kornfield for providing polymer samples. We thank Frank Weinhold and Scott Tobias for performing the *ab initio* calculations.

Supporting Information Available: ^2H T_1 data for deuterons in the 1,2-polybutadiene side group (3 pages). Ordering information is given on any current masthead page.

References and Notes

- (1) Kramers, H. A. *Physica* **1940**, *7*, 284.
- (2) Helfand, E. *J. Chem. Phys.* **1971**, *54*, 4651.
- (3) Glowinkowski, S.; Gisser, D. J.; Ediger, M. D. *Macromolecules* **1990**, *23*, 3520.
- (4) Zhu, W.; Gisser, D. J.; Ediger, M. D. *J. Polym. Sci., Polym. Phys. Ed.* **1994**, *32*, 2251.
- (5) Dejean de la Batie, R.; Laupretre, F.; Monnerie, L. *Macromolecules* **1988**, *21*, 2045.

- (6) Dejean de la Batie, R.; Laupretre, F.; Monnerie, L. *Macromolecules* **1989**, *22*, 122.
- (7) Gisser, D. J.; Glowinkowski, S.; Ediger, M. D. *Macromolecules* **1991**, *24*, 4270.
- (8) Dejean de la Batie, R.; Laupretre, F.; Monnerie, L. *Macromolecules* **1988**, *21*, 2052.
- (9) Spyros, A.; Dais, P.; Heatley, F. *Macromolecules* **1994**, *27*, 5845.
- (10) Lodge, T. P. *J. Phys. Chem.* **1993**, *97*, 1480.
- (11) Gisser, D. J.; Ediger, M. D. *Macromolecules* **1992**, *25*, 1284.
- (12) Schrag, J. L.; Stokich, T. M.; Strand, D. A.; Merchak, P. A.; Landry, C. J. T.; Radtke, D. R. *J. Non-Cryst. Solids* **1991**, *131*, 537.
- (13) Amelar, S.; Krahn, J. R.; Hermann, K. C.; Morris, R. L.; Lodge, T. P. *Spectrochim. Acta Rev.* **1991**, *14*, 379.
- (14) Floudas, G.; Fytas, G.; Brown, W. J. *J. Chem. Phys.* **1992**, *96*, 2164.
- (15) Rizos, A.; Fytas, G.; Lodge, T. P.; Ngai, K. L. *J. Chem. Phys.* **1991**, *95*, 2980.
- (16) Chung, G.-C.; Kornfield, J. A.; Smith, S. D. *Macromolecules* **1994**, *27*, 964.
- (17) Heatley, F. *Annu. Rep. NMR Spectrosc.* **1986**, *17*, 179 and references therein.
- (18) Heatley, F. *Prog. Nucl. Magn. Reson. Spectrosc.* **1979**, *13*, 47; and references therein.
- (19) Viswanath, D. S.; Natarajan, G. *Data Book on the Viscosity of Liquids*; Hemisphere Publishing: New York, 1989.
- (20) Rossini, F. D.; Pitzer, K. S.; Arnett, R. L.; Brawn, R. M.; Pimentel, G. C. *Selected Values of Physical and Thermodynamic Properties of Hydrocarbons and Related Compounds*; Carnegie Press: Pittsburgh, PA, 1953.
- (21) Stephan, K.; Lucas, K. *Viscosity of Dense Fluids*; Plenum Press: New York, 1979.
- (22) Merchak, P. A. Ph.D. Thesis, University of Wisconsin, 1987.
- (23) Landolt-Bornstein, *Zahlenwerte und Funktionen*; Springer-Verlag: Berlin, 1969; Band II, Teil 5, p 217.
- (24) Gronski, W.; Schaefer, T.; Peter, R. *Polym. Bull.* **1979**, *1*, 319.
- (25) Pham, Q. T.; Petiaud, R.; Waton, H. *Proton and Carbon NMR Spectra of Polymers*; John Wiley and Sons: Chichester, 1983.
- (26) Bovey, F. A. *Nuclear Magnetic Resonance Spectroscopy*, 2nd ed.; Academic Press: San Diego, CA, 1988.
- (27) Abragam, A. *The Principles of Nuclear Magnetism*; Clarendon Press: Oxford, 1961; Chapter VIII.
- (28) Loewenstein, A. *Advances in Nuclear Quadrupole Resonance*; John Wiley & Sons: London, New York, 1983; Vol. 5.
- (29) Lucken, E. A. C. *Nuclear Quadrupole Coupling Constants*; Academic Press: London, New York, 1969.
- (30) Often the correlation time is given the symbol τ_c . Here $\langle \sigma \rangle$ is used to represent the time integral of the correlation function. This is to emphasize that the integral is a model independent quantity. Note that $\langle \sigma \rangle$ is *not* the average value of the chemical shift.
- (31) Dais, P.; Spyros, A. Submitted to *Prog. Nucl. Magn. Reson. Spectrosc.*
- (32) Bovey, F. A.; Jelinski, L. W. *J. Phys. Chem.* **1985**, *89*, 571 and references therein.
- (33) Matsuo, K.; Stockmayer, W. H.; Mashimo, S. *Macromolecules* **1982**, *15*, 606.
- (34) Cais, R. E.; Bovey, F. A. *Macromolecules* **1977**, *10*, 752.
- (35) Cais, R. E.; Bovey, F. A. *Macromolecules* **1977**, *10*, 169.
- (36) Hatada, K.; Kitayama, T.; Terawaki, Y.; Tanaka, Y.; Sato, H. *Polym. Bull. (Berlin)* **1980**, *2*, 791.
- (37) Gronski, W.; Murayama, N. *Makromol. Chem.* **1976**, *177*, 3017.
- (38) Mashimo, S. *Macromolecules* **1976**, *9*, 91.
- (39) Lang, M. C.; Laupretre, F.; Noel, C.; Monnerie, L. *J. Chem. Soc., Faraday Trans.* **1979**, *275*, 349.
- (40) This is supported by fully optimized *ab initio* RHF/6-31G* calculations. These calculations indicate that the lowest energy barrier for the lowest energy conformational state in $\text{RCH}_2\text{CR}(\text{CH}=\text{CH}_2)$ is 14–15 kJ/mol when $\text{R} = \text{H}$ or CH_3 .
- (41) Adolf, D. B.; Ediger, M. D.; Kitano, T.; Ito, K. *Macromolecules* **1992**, *25*, 867.
- (42) Bagchi, B.; Oxtoby, D. *J. Chem. Phys.* **1983**, *78*, 2735.
- (43) See figure 7 in: Adolf, D. B.; Ediger, M. D. *Macromolecules* **1991**, *24*, 5834.
- (44) Compare Tables 2 and 5 in: Smith, G. D.; Yoon, D. Y.; Zhu, W.; Ediger, M. D. *Macromolecules* **1994**, *27*, 5563.
- (45) Moe, N. E.; Ediger, M. D. *Macromolecules* (to be submitted).
- (46) Cole, K. S.; Cole, R. H. *J. Chem. Phys.* **1941**, *9*, 341.
- (47) Schaefer, J. *Macromolecules* **1974**, *6*, 882.
- (48) Fuoss, R. M.; Kirkwood, J. G. *J. Am. Chem. Soc.* **1941**, *63*, 385.
- (49) Hail, C. K.; Helfand, E. *J. Chem. Phys.* **1982**, *77*, 3275.
- (50) Jones, A. A.; Stockmayer, W. H. *J. Polym. Sci. Polym. Phys. Ed.* **1977**, *15*, 847.
- (51) For example, Denault, J.; Prud'homme, J. *Macromolecules* **1989**, *22*, 1307.
- (52) Guillermo, A.; Dupeyre, R.; Cohen-Addad, J. P. *Macromolecules* **1990**, *23*, 1291.
- (53) The equations which describe the relaxation time distributions are collected in ref 7.
- (54) Kanaya, T.; Kaji, K.; Inoue, K. *Macromolecules* **1991**, *24*, 1826.
- (55) Howarth, O. W. *J. Chem. Soc. Faraday Trans. 2* **1980**, *76*, 1219.
- (56) Moe, N. E.; Ediger, M. E. *Macromolecules* **1995**, *28*, 2329.
- (57) Moe, N. E.; Ediger, M. D. *Polymer* (in press).
- (58) Gisser, D. J.; Ediger, M. D. *J. Phys. Chem.* **1993**, *97*, 10818.
- (59) Radiotis, T.; Brown, G. R.; Dais, P. *Macromolecules* **1993**, *26*, 1445.
- (60) Inoue, Y.; Konno, T. *Polym. J.* **1976**, *8*, 457.
- (61) Gronski, W.; Murayama, N. *Makromol. Chem.* **1978**, *179*, 1509.
- (62) Spyros, A.; Dais, P.; Heatley, F. *Macromolecules* **1994**, *27*, 6207.
- (63) Dejean de la Batie, R.; Laupretre, F.; Monnerie, L. *Macromolecules* **1989**, *22*, 2617.

MA950506F